

# Criticality and factorization in the Heisenberg chain with Dzyaloshinskii-Moriya interaction

Tian-Cheng Yi,<sup>1,2</sup> Wen-Long You,<sup>1,2,\*</sup> Ning Wu,<sup>3</sup> and Andrzej M. Oleś<sup>4,5</sup>

<sup>1</sup>College of Science, Nanjing University of Aeronautics and Astronautics, Nanjing, 211106, China

<sup>2</sup>School of Physical Science and Technology, Soochow University, Suzhou, Jiangsu 215006, China

<sup>3</sup>Center for Quantum Technology Research, School of Physics, Beijing Institute of Technology, Beijing 100081, China

<sup>4</sup>Max Planck Institute for Solid State Research, Heisenbergstrasse 1, D-70569 Stuttgart, Germany

<sup>5</sup>Marian Smoluchowski Institute of Physics, Jagiellonian University, Prof. S. Łojasiewicza 11, PL-30348 Kraków, Poland

(Dated: 31 May 2019)

In this work, we address the ground state properties of the anisotropic spin-1/2 Heisenberg XYZ chain under the interplay of magnetic fields and the Dzyaloshinskii-Moriya (DM) interaction which we interpret as an electric field. The identification of the regions of enhanced sensitivity determines criticality in this model. We calculate the Wigner-Yanase skew information (WYSI) as a coherence witness of an arbitrary two-qubit state under specific measurement bases. The WYSI is demonstrated to be a good indicator for detecting the quantum phase transitions. The finite-size scaling of coherence susceptibility is investigated. We find that the factorization line in the antiferromagnetic phase becomes the factorization volume in the gapless chiral phase induced by DM interactions, implied by the vanishing concurrence for a wide range of field. We also present the phase diagram of the model with three phases: antiferromagnetic, paramagnetic, and chiral, and point out a few common mistakes in deriving the correlation functions for the systems with broken reflection symmetry.

## I. INTRODUCTION

Quantum phase transitions (QPTs) that deal with dramatic changes of the ground state and low-excitation properties induced by small variations of driving parameters, are one of very active fields of research in several contexts of modern statistical mechanics, quantum information, and condensed matter physics. QPTs are believed to take place exclusively in many-body systems [1], while it has been recently realized that a few-body system may also develop a QPT [2–6]. Quantum fluctuation accumulated by the non-commutativity between the driving term and the rest are responsible for the sudden change of the correlations among the system's constituents.

In view of the central role played in interdisciplinary fields, it is of crucial importance to devise suitable tools for a proper characterization of the changes of a quantum system at a QPT. To this purpose, different quantum-information-based concepts have been put forward over recent years, in order to identify ground-state variations across QPTs. Quantum coherence and quantum entanglement are two characteristic properties of a quantum system. Both of them are considered to be valuable resources in most quantum information processing tasks [7–11]. Quantum entanglement indicates that a quantum state is nonseparable and was first pointed out by Schrödinger in 1935 for constituent subsystems [12]. Furthermore, entanglement spectrum is very useful in recognizing certain QPTs in spin systems [13]. In contrast, quantum coherence concerns the set of states and is usually defined in a given basis by measuring the distance

between the quantum state  $\rho$  and its closest incoherent state for the system as a whole [14]. Although these two quantum mechanical properties have a completely different origin, indications exist that they are equivalent by computing [15].

It is known that the correlation length tends to be infinite in the critical regime although the interactions are short-ranged, which can lead to diverging susceptibilities signalling a QPT. The sensitivity is greatly enhanced especially for the system at the quantum criticality comparing with that away from the critical region. In this respect, quantum-enhanced measurements open the path to many new forms of enhanced sensitivity across the quantum criticality [16]. Taking external fields as probes, the sensitivity given by the entanglement susceptibility, coherence susceptibility [17, 18], and fidelity susceptibility [19, 20] infers the signatures of quantum critical points and scaling behaviors. Such strategy is very useful in Hamiltonian engineering, when one can evaluate the effect of added terms in the Hamiltonian.

To investigate the quantum criticality, we consider a specific quasi-classical ground state that can be modulated in the anisotropic quantum antiferromagnetic (AFM) chain under external fields, as pointed by the pioneering work of Kurmann, Thomas, and Müller [21]. The separable states are namely the free states in the resource theory of entanglement [22]. The possible engineering of a completely separable state is nontrivial and particularly significant in the presence of strong interactions for information processes [23] and quantum simulation [24]. Over recent years, several physical quantities and experimental methods have been developed for identification and exploration of QPTs. In the last decade, quantum-information measures, such as in the form of entanglement and coherence, were found to be an effective

\* youwenlong@gmail.com

tool for characterizing QPTs and ground-state factorization. Exploring both criticality and factorization using the tools of quantum information has proven fruitful in a number of contexts, e.g., low-dimensional spin models, fermionic systems, cold atom system, and open quantum systems.

In this work, we focus on the one-dimensional (1D) Heisenberg model with nearest neighbor exchange coupling, which has long served as an archetype for the study of quantum magnetism in low dimensions. Strong fluctuations of interacting spins are of particular importance at low dimension, where the Mermin-Wagner theorem states that thermal fluctuations prevent long-range order at any finite temperature when the Hamiltonian obeys a continuous rotational symmetry in spin space. Even at absolute zero temperature, the zero-point fluctuations may also prevent long-range order by incorporating additional interactions. The effects induced by external electric and magnetic fields have been of particular interest since the magnetic state can be qualitatively different depending on the magnitude and direction of the external fields. This has led to interest in the study of QPTs at finite fields [25–27].

Recently, Radhakrishnan, Ermakov, and Byrnes [28] studied the quantum coherence in the XY chain with Dzyaloshinsky-Moriya (DM) interaction and indicated that quantum Jensen-Shannon divergence can efficiently probe the second-order QPT. Moreover, the local and intrinsic ingredient among the total quantum coherence can be discriminated to characterize the first-order QPTs in spin-1/2 XXZ chain [29] and the topological QPTs in the extended XY model [30]. The QPTs and the quantum coherence in Heisenberg XYZ systems were not investigated carefully until now. While most studies consider the ground-state factorization in symmetric spin system, the knowledge is lacking in wondering the existence of factorized ground states in more complex multipartite systems. The primary motivation of the present work is to try to elucidate the role of DM interaction in Heisenberg XYZ model, and explore whether quantum criticality and factorization can be captured by emerging coherence. Exploiting favorable figures of merit of quantum information measures allows extracting the full ground-state phase diagram of the spin-1/2 Heisenberg XYZ chain. We remark that especially two-qubit reduced density matrices adopted in Ref. [28] are improper.

The remainder of this paper is organized as follows. We introduce the 1D anisotropic Heisenberg model with DM interactions in Sec. II. In Sec. III, we present the analytical approach and calculate quantum entanglement and quantum coherence. In Sec. IV, we discuss the scaling behavior of the local quantum coherence in the XY model, and the factorization phenomena under the interplay of DM interactions and magnetic field. Finally, in Sec. V we give the summary and conclusion.

## II. THE MODEL

We consider the anisotropic Heisenberg chain described by the following Hamiltonian:

$$\mathcal{H} = J \sum_{j=1}^N \left( \frac{1+\gamma}{2} \sigma_j^x \sigma_{j+1}^x + \frac{1-\gamma}{2} \sigma_j^y \sigma_{j+1}^y + \Delta \sigma_j^z \sigma_{j+1}^z \right) + \sum_{j=1}^N \vec{D} \cdot (\vec{\sigma}_j \times \vec{\sigma}_{j+1}) - h \sum_{j=1}^N \sigma_j^z, \quad (1)$$

where  $N$  is the number of the spins in the chain, and the periodic boundary condition is assumed, i.e.,  $\vec{\sigma}_{N+j} = \vec{\sigma}_j$ , and  $\vec{\sigma}_j = \{\sigma_j^x, \sigma_j^y, \sigma_j^z\}$ . The model has AFM exchange coupling ( $J \geq 0$ ), anisotropy  $\Delta$ , DM vector  $\vec{D}$ , and uniform magnetic field strength  $h$  acting on  $\{\sigma_j^z\}$ . Here we presume that the  $\vec{D}$  vector is along the direction perpendicular to the plane, i.e.,  $\vec{D} = D\hat{z}$  and we take  $D$  as a unit of  $\vec{D}$ . The parameter  $\gamma \geq 0$  measures the anisotropy of spin-spin interactions in the  $xy$  plane which typically varies from 0 (isotropic XY model) to 1 (Ising model).

Several types of model interactions are currently being explored for simulating effective spin systems like Ising, XY, and XYZ, which may stand for systems of trapped ions [31] or polaritons [32]. An important extension of the effective models is the DM interaction which can be interpreted as an electric field. The DM interaction was introduced by Dzyaloshinskii and Moriya in a phenomenological model [33] and a microscopic model [34], respectively. The DM interactions exist in solids, such as ferrimagnetic insulator  $\text{Cu}_2\text{OSeO}_3$  [35–37] or multiferroic  $\text{BiFeO}_3$  [38], and are synthesized in optical lattices for both fermions [39, 40] and bosons [41, 42].

A microscopic mechanism arises from that the electric polarization generated by the displacement of oppositely charged ions is driven by non-collinear spiral magnetic structures with a cycloidal component as described by Tokura [43],  $\vec{P} \propto \hat{e}_{ij} \times (\vec{\sigma}_i \times \vec{\sigma}_j)$ , where  $\hat{e}_{ij}$  is the unit vector connecting the neighboring spins  $\vec{\sigma}_i$  and  $\vec{\sigma}_j$ . The coupling coefficient of macroscopic polarization is material-dependent [44], and the sign depends on the vector spin chirality. In this respect, an energy shift,  $-\vec{D} \cdot \vec{P}$ , by applying an electric field  $\vec{D}$  prevails over the Heisenberg exchange and the QPT occurs in this system. The supplemented DM interaction can be gauged away by performing a spin rotation with respect to a twist phase,  $\phi = \tan^{-1}(D/J)$  of spin operators,  $\sigma_j^+ \sigma_{j+1}^- \rightarrow \sigma_j^+ \sigma_{j+1}^- e^{i\phi}$ , for  $\gamma = 0$  [45]. So, in this way the XXZ model has been changed to the XYZ model after rotation. Note that the absence of inversion symmetry in DM interaction introduces anisotropy to the system.

## III. THE INFORMATION MEASURES

For general parameters, Hamiltonian (1) is not integrable except at specific points in parameter space. In

the case of  $\gamma = 0$ ,  $D = 0$ ,  $h = 0$ , one finds that the XXZ spin chain with nearest neighbor interaction is integrable, and it can be analytically solved using the Bethe ansatz [46, 47]. Here we use Jordan-Wigner transformation to represent the spin operators  $\sigma_j^\pm = (\sigma^x \pm i\sigma^y)/2$  by fermion operators:

$$\sigma_j^+ = \exp \left[ i\pi \sum_{i=1}^{j-1} c_i^\dagger c_i \right] c_j = \prod_{i=1}^{j-1} \sigma_i^z c_j, \quad (2)$$

$$\sigma_j^- = \exp \left[ -i\pi \sum_{i=1}^{j-1} c_i^\dagger c_i \right] c_j^\dagger = \prod_{i=1}^{j-1} \sigma_i^z c_j^\dagger, \quad (3)$$

$$\sigma_j^z = 1 - 2c_j^\dagger c_j. \quad (4)$$

For  $\Delta \neq 0$ , we approximate the model (1) by mean-field decoupling [48]. In this approximation, the Ising coupling (four-fermion interaction) is decomposed into three mean-field channels using Wick's theorem, which are determined self-consistently in the noninteracting system:

$$\begin{aligned} & c_j^+ c_j c_{j+1}^+ c_{j+1} \\ & \approx \langle c_j^+ c_j \rangle c_{j+1}^+ c_{j+1} + \langle c_{j+1}^+ c_{j+1} \rangle c_j^+ c_j - \langle c_j^+ c_j \rangle \langle c_{j+1}^+ c_{j+1} \rangle \\ & - \langle c_j^+ c_{j+1}^+ \rangle c_j c_{j+1} - \langle c_j c_{j+1} \rangle c_j^+ c_{j+1}^+ + \langle c_j^+ c_{j+1}^+ \rangle \langle c_j c_{j+1} \rangle \\ & + \langle c_j^+ c_{j+1} \rangle c_j c_{j+1}^+ + \langle c_j c_{j+1}^+ \rangle c_j^+ c_{j+1} - \langle c_j^+ c_{j+1} \rangle \langle c_j c_{j+1}^+ \rangle. \end{aligned} \quad (5)$$

We mainly use the mean-field approximation of the translation invariant Hamiltonian to get the three self-consistent parameters  $\{\mu, t, \delta\}$  (see below),

$$\begin{aligned} \mathcal{H} &= \sum_{j=1}^N \{ [Jc_{j+1}^+ c_j + J\gamma c_{j+1}^+ c_j^+ + \text{h.c.}] \\ & + J\Delta(1 - 2c_j^+ c_j)(1 - 2c_{j+1}^+ c_{j+1}) - h(1 - 2c_j^+ c_j) \} \\ & \approx \sum_{j=1}^N \{ [(t + 2iD)c_{j+1}^+ c_j + \delta c_j^+ c_{j+1}^+ + \text{h.c.}] + \mu c_j^+ c_j \} \\ & + \text{const}, \end{aligned} \quad (6)$$

i.e.,  $\mu = 4J\Delta(2\langle c_j^+ c_j \rangle - 1) + 2h$ ,  $t = J(1 - 4\Delta\langle c_j^+ c_{j+1} \rangle)$ , and  $\delta = J(\gamma - 4\Delta\langle c_j c_{j+1} \rangle)$ . The values of  $\{\mu, t, \delta\}$  can be determined self-consistently (see Appendix B).

First, we discuss the model Eq. (1) at  $\Delta = 0$ , where it reduces to the XY chain. The XY model is an archetypal model of quantum physics, encapsulating the physics underlying universal phenomena in equilibrium phase transition, much less looking for exotic phases through machine learning [49–56]. On one hand, the linear XY chain in the presence of transverse fields plays a central role in condensed matter theory [57, 58] and is a good candidate for building blocks in quantum computers [59, 60] and quantum information applications [61]. On the other hand, and maybe even more importantly, the XY model is one of few exactly solvable models in strongly correlated systems, and thus provides the benchmark for

other approximate techniques implemented in more realistic models, especially for the accurate calculation of various dynamic quantities.

While being relatively simple, the XY model exhibits a rich phase diagram. Applying the transverse field induces an Ising transition at  $h_c = 1$  from AFM phase to paramagnetic (PM) phase. Moreover, a completely factorized ground state may occur at a specific value of the field,

$$h_f = J \sqrt{\left( \frac{1+\gamma}{2} + \Delta \right) \left( \frac{1-\gamma}{2} + \Delta \right)}, \quad (7)$$

in the absence of DM interaction [62].

We are now in a position to explore the quantum coherence and entanglement measures based on the reduced density matrix. They can be determined without a full tomography of the state under consideration. The studies of quantum entanglement and coherence are crucial for both fundamental issues and niche technological applications. We consider the representation spanned by the two-qubit product states:  $|1\rangle \equiv |\uparrow\rangle_i \otimes |\uparrow\rangle_j$ ,  $|2\rangle \equiv |\uparrow\rangle_i \otimes |\downarrow\rangle_j$ ,  $|3\rangle \equiv |\downarrow\rangle_i \otimes |\uparrow\rangle_j$ , and  $|4\rangle \equiv |\downarrow\rangle_i \otimes |\downarrow\rangle_j$ . Here  $|\uparrow\rangle$  ( $|\downarrow\rangle$ ) stands for spin up (down) state, and the reduced density matrix for selected two auxiliary qubits can be expressed in the following form:

$$\rho_{ij} = \begin{pmatrix} u^+ & 0 & 0 & z_1 \\ 0 & w_1 & z_2 & 0 \\ 0 & z_2^* & w_2 & 0 \\ z_1^* & 0 & 0 & u^- \end{pmatrix}, \quad (8)$$

with

$$u^\pm = \frac{1}{4} (1 \pm 2\langle \sigma_i^z \rangle + \langle \sigma_i^z \sigma_j^z \rangle), \quad (9)$$

$$z_1 = \frac{1}{4} (\langle \sigma_i^x \sigma_j^x \rangle - \langle \sigma_i^y \sigma_j^y \rangle - i\langle \sigma_i^x \sigma_j^y \rangle - i\langle \sigma_i^y \sigma_j^x \rangle), \quad (10)$$

$$z_2 = \frac{1}{4} (\langle \sigma_i^x \sigma_j^x \rangle + \langle \sigma_i^y \sigma_j^y \rangle + i\langle \sigma_i^x \sigma_j^y \rangle - i\langle \sigma_i^y \sigma_j^x \rangle), \quad (11)$$

$$\omega_1 = \omega_2 = \frac{1}{4} (1 - \langle \sigma_i^z \sigma_j^z \rangle). \quad (12)$$

A representative state  $X$  stands for a five-parameter family of states of two qubits. Be aware that the reflection symmetry is broken in Hamiltonian (1) thanks to the existence of DM terms. In this case,  $\langle \sigma_i^x \sigma_j^y \rangle$  and  $\langle \sigma_i^y \sigma_j^x \rangle$  in Eqs. (10) and (11) are not necessarily vanishing, see Fig. 1(a). Nevertheless, a simplification that  $\langle \sigma_i^x \sigma_j^y \rangle = 0$  and  $\langle \sigma_i^y \sigma_j^x \rangle = 0$  was commonly used in the past [28, 63–65]. Also, such negligence in calculating Eqs. (9) and (12) frequently occur in terms of the relation [28, 63–65]:

$$\begin{aligned} \langle \sigma_j^z \sigma_{j+1}^z \rangle &= \langle \sigma_j^z \rangle \langle \sigma_{j+1}^z \rangle - \langle \sigma_j^x \sigma_{j+1}^x \rangle \langle \sigma_j^y \sigma_{j+1}^y \rangle \\ &+ \langle \sigma_j^x \sigma_{j+1}^y \rangle \langle \sigma_j^y \sigma_{j+1}^x \rangle. \end{aligned} \quad (13)$$

As is shown in Fig. 1(b), the inclusion of the last term in Eq. (13) brings a prominent difference. For instance, the first-derivative of nearest neighbor correlation accurately

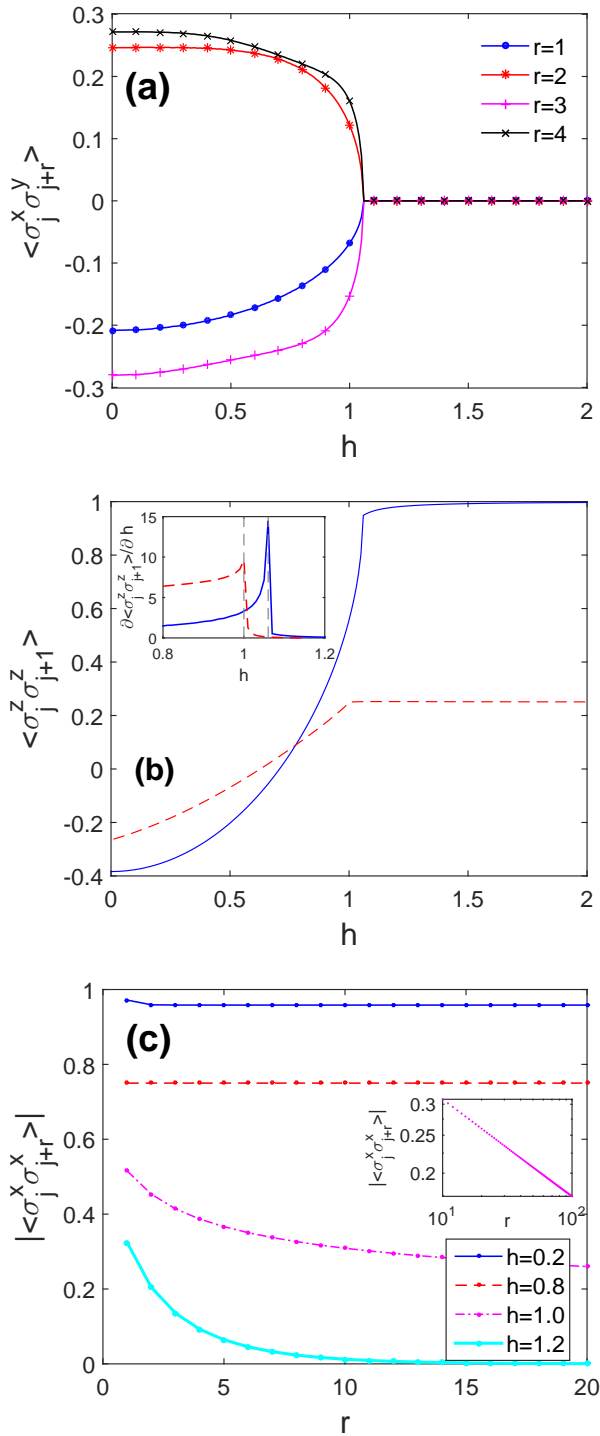


FIG. 1. Short-range correlations for increasing field  $h$ : (a) two-qubit correlations  $\langle \sigma_j^x \sigma_{j+r}^y \rangle$  for different distance with  $\gamma = 0.2$ , and (b) the nearest neighbor correlation,  $\langle \sigma_j^z \sigma_{j+1}^z \rangle$  with  $\gamma = 0.2$ . The solid line is plotted according to Eq. (13), while the dashed line is obtained by assuming  $\langle \sigma_j^x \sigma_{j+1}^y \rangle = 0$ . Inset shows the corresponding first derivative. (c) The absolute value of the correlation function,  $|\langle \sigma_j^x \sigma_{j+r}^x \rangle|$  with  $\gamma = 0.6$ , for increasing  $r$ . Other parameters:  $D = 0.2$ ,  $\Delta = 0$ ,  $J = 1$ .

discriminates the criticality. A two-qubit state tomography can be implemented on the system qubits [66], and holds advantage that a full tomography of the state is not necessary.

Quantum coherence is a kind of quantification of quantum superposition, which is one of the most significant properties of quantum states separate from classical ones. As the core of quantum physics and quantum information, there are many important applications in various quantum tasks, such as quantum computation and quantum communication. There are many related studies [18, 28, 64, 67, 68]. A well-defined and frequently used coherence measure is Wigner-Yanase skew information (WYSI), which has some clear physical meanings, such as it is equal to the optimal distillation rate for standard coherence distillation, and can also be interpreted as the minimal amount of noise required to achieve full decoherence of the state under discussion. WYSI mainly quantifies the information encapsulated in a quantum state with respect to an observable  $K$  [69, 70], which has implemental value in both theoretical and experimental schemes in view of the current technology:

$$\mathcal{I}(\rho, K) = -\frac{1}{2} \text{Tr}[\sqrt{\rho}, K]^2, \quad (14)$$

where  $[..]$  stands for the commutator. The WYSI was interpreted as a measure quantifying the non-commutativity between  $\rho$  and  $K$  [71], and thus captures the genuine quantum uncertainty of a given observable in a certain quantum state. Very recently it has been proven by Girolami [70] that  $\mathcal{I}(\rho, K)$  given by Eq. (14) satisfies all the criteria for coherence monotones [14] and consequently can be used as a reliable measure of coherence.

We find that the QPT and factorization phenomenon are both associated with the local quantum coherence (LQC) [30, 72], as quantified by WYSI, in single-spin and two-spin reduced density matrices of the ground state of the spin chain. For a bipartite system, the LQC describes the observable that acts only on one of the subsystems, as  $\mathcal{I}(\rho_{AB}, K_A \otimes I_B)$ . Here we choose  $K_A$  as  $\sigma^x$  or  $\sigma^z$ . Karpat, Cakmak, and Franchini found that the WYSI remains non-increasing under classical mixing of quantum states [72]. It filters out the pure quantum uncertainty in a measurement.

The absence of the WYSI implies that no quantum uncertainty can be observed, and statistical errors are due to classical ignorance. Analogously, the concurrence is a pairwise entanglement measure for any bipartite system that relates to the two-site reduced density matrix  $\rho$  [73]. The concurrence for a two-qubit state  $\rho_{ij}$  is defined as  $C=2 \max\{0, \Lambda_1, \Lambda_2\}$ , where  $\Lambda_1 = |z_1| - \sqrt{\omega_1 \omega_2}$  and  $\Lambda_2 = |z_2| - \sqrt{u^+ u^-}$  [74].

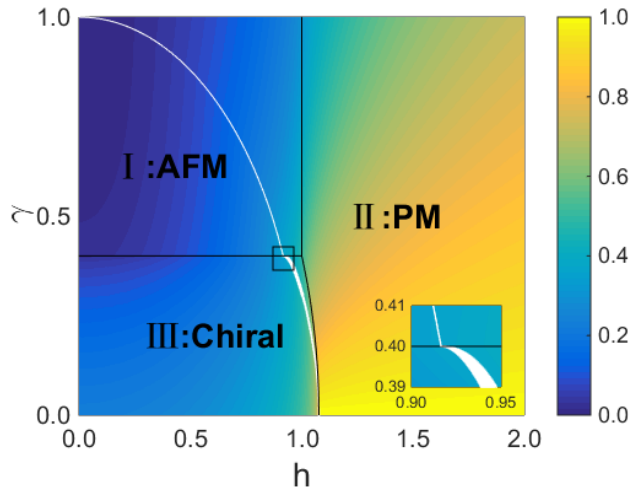


FIG. 2. Magnetic phase diagram of the 1D XY model with three (black solid) lines separating the phases I, II, and III. In the special case of  $D = 0$ , the chiral phase vanishes. The color map represents the strength of the LQC $_x$ ,  $\mathcal{I}(\rho_{j,j+1}, \sigma_j^x)$ . The white zone in the AFM phase and the chiral phase delegates the factorization line and the factorization region, respectively. Parameter:  $D = 0.2$ ,  $\Delta = 0$ , and  $J = 1$ .

#### IV. RESULTS

To understand better the ground state in different regimes of parameters it is natural to utilize diverse quantum information measures to unfold the landscape of the criticality and factorization under the effect of DM interactions and  $\Delta$ . In order to fully appreciate the diversity of solutions, it is sufficient to study the special cases with the spin-spin interactions in the  $xy$  plane. For  $\Delta = 0$ , the diagonalization procedure of the left flip-flop couplings can be achieved by the well-established techniques including Jordan-Wigner, Fourier, and Bogoliubov transformations (see Appendix A). Using the exact solutions, the correlation functions could be obtained, and the magnetic phase diagram presented in Fig. 2 was found.

The phase diagram consists of three phases: AFM phase I, PM phase II, and gapless Chiral phase III. The phase boundaries are determined by three lines:  $h = 1$ ,  $\gamma = 2D$ , and  $h = \sqrt{4D^2 - \gamma^2 + 1}$ , respectively [75]. As shown in Fig. 1(c), in the AFM phase, the correlation function  $\langle \sigma_i^x \sigma_{i+r}^x \rangle$  becomes a constant quickly, although there is a small decrease for  $r \geq 2$  comparing with the nearest neighbor correlation. At the critical point, i.e., at  $h = 1.0$ , the correlation function has an algebraic decay, namely,  $\langle \sigma_i^x \sigma_{i+r}^x \rangle \sim r^{-1/4}$ . On the contrary, the correlation function decays exponentially with the increase of  $r$  in the PM phase.

Figure 3 examines the local quantum  $\sigma^x$  coherence (LQC $_x$ ) and the local quantum  $\sigma^z$  coherence (LQC $_z$ ) along  $\gamma = 0.6$  and  $\gamma = 0.2$ , respectively, with  $D = 0.2$ , which corresponds to AFM-PM and chiral-PM transitions. The LQC $_x$  is monotonously increasing with  $h$ , in

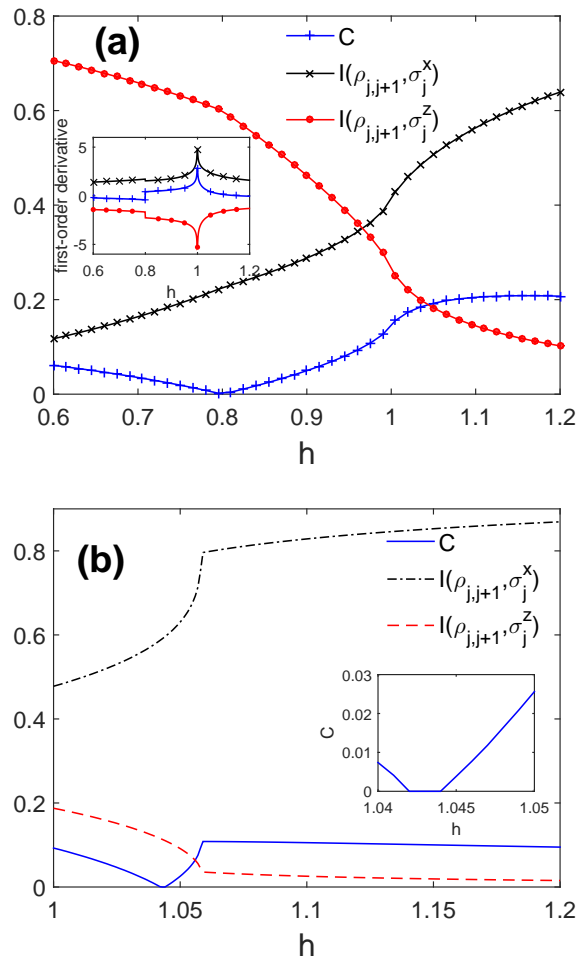


FIG. 3. The concurrence, LQC $_x$  and LQC $_z$  with respect to  $h$  at  $D = 0.2$ , and for: (a)  $\gamma=0.6$ ; (b)  $\gamma=0.2$ . Inset in (a) shows the first-derivative of the concurrence, LQC $_x$  and LQC $_z$ . Inset in (b) shows the magnified factorized zone. Parameter:  $\Delta = 0$ ,  $J = 1$ .

contrast to the monotonous decay of LQC $_z$ . The LQC $_x$  is indeed large for large  $h$ , especially for  $\gamma = 0$ , where LQC $_x$  dramatically increases to unity when  $h$  approaches  $h_c$ . Instead, the concurrence shows the non-monotonous characteristics of entanglement. As  $h$  increases, the concurrence firstly decreases to zero and then increases with  $h$ . Although the entanglement and coherence measures do not exhibit any divergences, the divergences of their first derivatives with respect to  $h$  may be used to identify the critical points. Indeed, the derivative of the quantum information measures has been proven to be a powerful tool to detect the location of the quantum critical points [76–82].

In the inset of Fig. 3(a), one observes that the first derivatives of both LQC $_x$  and LQC $_z$  show a cusp singularity at  $h_m$ , which marks the point of the QPT. It is even more evident in Fig. 3(b) that the critical points can be identified by kink behavior in these information

measures. In this case, their first derivatives are discontinuous. Note that the quantum Jensen-Shannon divergence was adopted to inspect the quantum coherence of the 1D XY model with DM interactions [28]. However, an incomplete phase diagram is identified due to the illegal results of  $\langle \sigma_i^x \sigma_j^y \rangle$ ,  $\langle \sigma_i^y \sigma_j^x \rangle$ ,  $\langle \sigma_i^z \sigma_j^z \rangle$  in the presence of DM interactions, as is clearly demonstrated in Fig. 1(a-b). We remark that  $\langle \sigma_i^x \sigma_j^y \rangle = 0$  and  $\langle \sigma_i^y \sigma_j^x \rangle = 0$  should not be taken for granted in general for a system with broken reflection symmetry.

Along with the location of quantum critical points, the critical exponents can also be extracted by the scaling of quantum information measures. The first-order derivatives of the two-spin local  $\sigma^z$  coherence with respect to  $h$  are shown in Fig. 4(a). We notice that the first-order derivative around the critical point becomes sharper and sharper as the system size increases, and it is expected to diverge in the thermodynamic limit. The first-order derivative of the LQC $_z$  follows a logarithmic divergence across the critical point,

$$\left(\frac{\partial \mathcal{I}}{\partial h}\right)_{\max} \propto k_1 \log_2 N, \quad (15)$$

as is disclosed in the inset of Fig. 4(a). Here  $k_1$  is a constant and is monotonically decreasing with  $\gamma$ .

We analyzed the relative entropy, the concurrence and the logarithmic negativity, and find their first-order derivatives obey similar logarithmic scalings with different  $k_1$ , which are consistent with the results in Refs. [57, 78]. However, for the QPT between gapless chiral phase and gapped PM phase, the derivatives of the LQC have pronounced peaks [see Fig. 4(b)] which appear independent of system size. The location of the pseudocritical field  $h_m$  approaches the true critical point  $h_c$  as  $N \rightarrow \infty$ . Due to the relevance of the driving Hamiltonian under the renormalization group transformation, the leading term in the expansion of pseudocritical point for sufficiently large systems obeys such scaling behavior as in Refs. [57, 78],

$$|h_m - h_c| \sim N^{-\alpha}. \quad (16)$$

By applying linear regression to the raw data obtained from  $\mathcal{I}(\rho_{i,i+1}, \sigma_i^z)$  on various system sizes, one obtains  $\alpha = 1.6642$  for  $\gamma = 1$ .

Alternately, slightly away from the critical point in the thermodynamic limit, the first field derivative of  $\mathcal{I}$  satisfies,

$$\left(\frac{\partial \mathcal{I}}{\partial h}\right) \sim k_2 \log_2 |h - h_c|. \quad (17)$$

According to the scaling *Ansatz* for logarithmic scaling [83], the ratio of  $|k_1/k_2|$  gives rise to the correlation length exponent  $\nu$ . Similar results were obtained as well by the earlier studies [57, 78, 84]. The values resulting from different measures are consistent with each other up to two digits [85]. The results for  $\gamma = 0.6$  and 1.0, with  $D = 0.2$ , are listed in Table I, which suggests  $\nu \simeq 1$  for Ising transition.

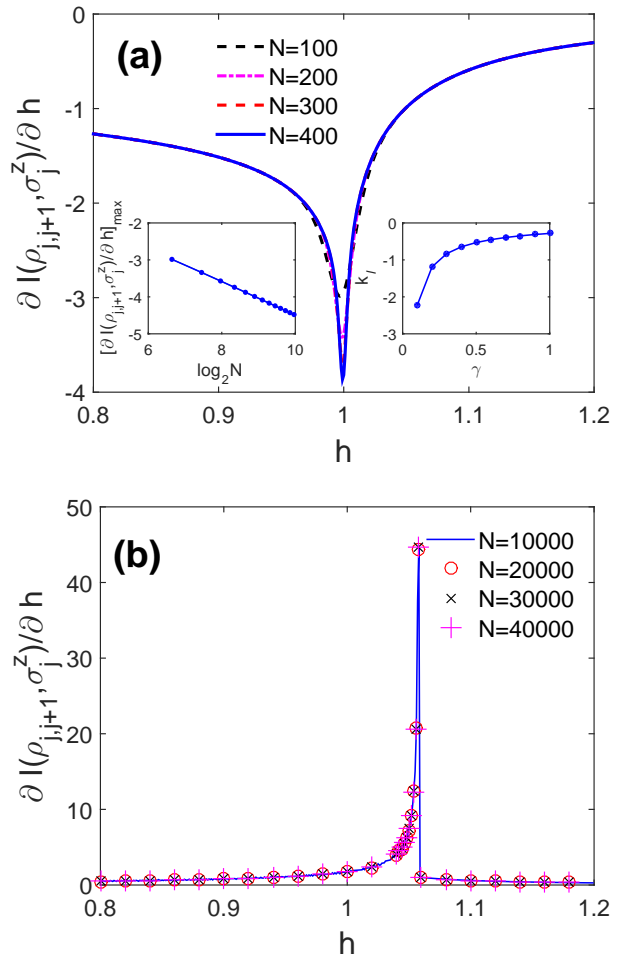


FIG. 4. The first derivative of LQC $_z$  with respect to  $h$  for different system sizes with: (a)  $\gamma=0.6$ , and (b)  $\gamma=0.2$ . In the left inset of (a), the maxima of the peaks (dots) follow a logarithmic scaling  $(\frac{\partial \mathcal{I}}{\partial h})_{\max} = 0.382 \log_2 N - 0.056$  (solid line). The right inset shows the dependence of  $k_1$  in Eq. (15) on  $\gamma$ . Other parameters:  $D = 0.2$ ,  $\Delta = 0$ , and  $J = 1$ .

A close inspection of Fig. 3(a) reveals there is an interesting phenomenon simultaneously at  $h_f = 0.8$ , where the concurrence becomes zero and the LQC has a jump

TABLE I. Fitting parameters  $\{k_1, k_2, \nu\}$  of the slope in logarithmic scaling across the critical points with  $D = 0.2$ ,  $\Delta = 0$ , and  $J = 1$ .

$\gamma$	parameter	$C$	$\mathcal{I}(\rho_{j,j+1}, \sigma_j^z)$
0.6	$k_1$	0.33813	0.45847
	$k_2$	-0.33893	0.44162
	$\nu$	0.99764	1.03815
1.0	$k_1$	0.18655	0.28532
	$k_2$	-0.18548	0.30575
	$\nu$	0.99426	1.07160

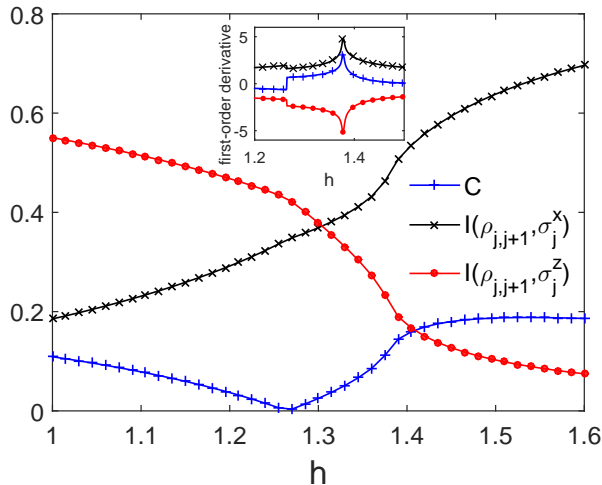


FIG. 5. The concurrence,  $LQC_x$  and  $LQC_z$  with respect to  $h$ . Inset shows their first-derivative. Parameters:  $\gamma = 0.6$ ,  $D = 0.2$ ,  $\Delta = 0.2$ , and  $J = 1$ .

discontinuity. The null point of the concurrence implies the ground state is disentangled at this point, where the ground state simplifies into simple product states, i.e.,  $|\psi_0\rangle = \prod_{i=1}^N \otimes |\psi_i\rangle$ , where  $|\psi_i\rangle$  are the states of the spins on the  $i$ th site. Such product states lie exactly on a classical line  $\gamma^2 + h^2 = 1$  in the absence of the interaction  $\propto D$  [21, 86, 87], where the intersite correlations are independent of the distance  $r$  of two qubits, see Fig. 1(c).

As such, we find the logarithmic negativity is also able to mark the classical feature while the von Neumann entropy fails to spot vanishing entanglement. Notice that ground states of interacting spin systems in the presence of an external magnetic field are typically entangled and a completely separable ground state emerges only under strict conditions. The exceptional phenomenon of separable ground state has been thoroughly investigated in spin systems immersed in a uniform transverse field [62, 88, 89], and nonuniform field [90, 91]. It was recognized that the factorization is a consequence of ground-state parity transition. Moreover, the behavior of the correlation functions changes from monotonic decay to oscillatory tail across the factorization point [92]. On this line, by examining the ground state of finite-size systems, the coherence and entanglement witness remain constant for all values of  $r$  at  $h_f$  in the thermodynamic limit, when the system is actually in the Néel phase [86].

In the chiral phase, shown in Fig. 3(b), the concurrence also exhibits a similar trend with the increase of  $h$ . It is odd to find that in this case the concurrence is vanishing for a finite range of  $h$ . In addition, the range gets narrower as  $\gamma$  decreases. The factorization volume in chiral phase is connected with the factorization line in the AFM phase across the critical boundary  $\gamma = 2D$ , as displayed in the inset of Fig. 2. Also, the correlation functions are not constant anymore, and instead, the amplitude

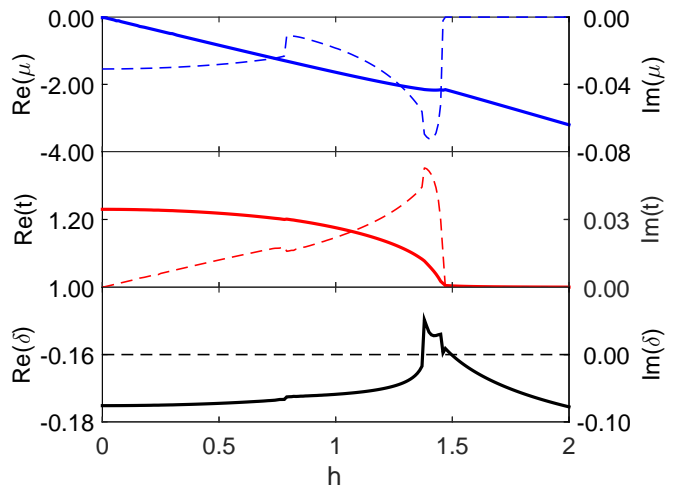


FIG. 6. Self-consistent mean-field parameters  $\mu$ ,  $t$ , and  $\delta$  as a function of  $h$  for  $\Delta = 0.2$ ,  $D = 0.2$ ,  $\gamma = 0.2$ , and  $J = 1$ . The solid lines correspond to the real parts, while the dotted lines represent the imaginary parts.

of correlation functions, including  $\langle \sigma_i^x \sigma_{i+r}^x \rangle$ ,  $\langle \sigma_i^x \sigma_{i+r}^y \rangle$ , shows oscillating decrease. Surprisingly, the coherence measures, including  $\mathcal{I}(\rho_{i,i+r}, \sigma_i^x)$  and  $\mathcal{I}(\rho_{i,i+r}, \sigma_i^z)$ , exhibit a smooth decay. The first derivative of the local coherence  $\mathcal{I}(\rho_{ij}, \sigma_i^x)$  correctly spotlights the location of the second-order QPT at  $h_c = \sqrt{4D^2 - \gamma^2 + 1}$  through a divergence, but no sign of the nontrivial factorization region can be observed.

To proceed, we examine the relation between the quantum-information quantifier with QPTs in the presence of anisotropy term  $\Delta$ . For axial regime  $\Delta \gg 1$  ( $\Delta \ll -1$ ), the system effectively stays in the Néel (fer-

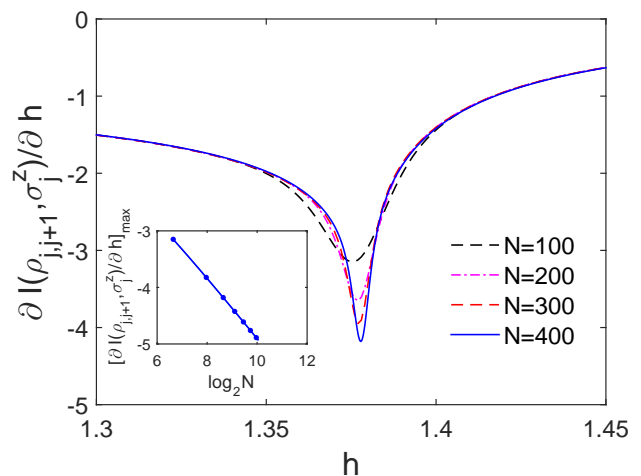


FIG. 7. The first-derivative of  $LQC_z$  with respect to  $h$  for different system sizes with  $\gamma=0.6$ ,  $D=0.2$ ,  $\Delta=0.2$ , and  $J = 1$ . Inset shows the relation between maxima of the peaks and the logarithm of system size  $N$ .



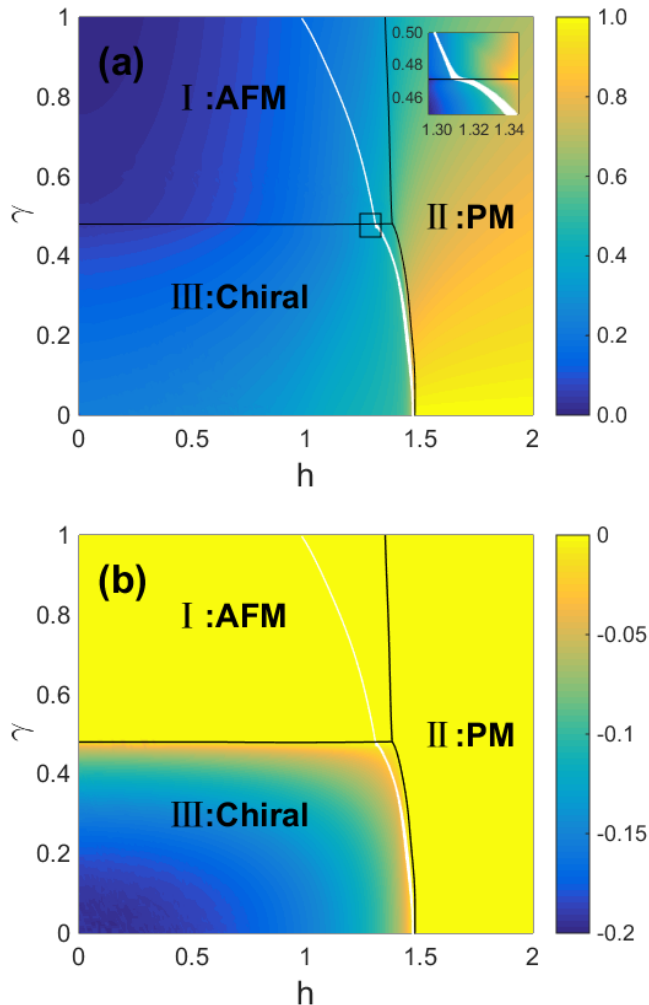


FIG. 8. Different parameter regimes of the 1D Heisenberg model in the  $(h, \gamma)$  plane obtained: (a) phase diagram; the color map represents the strength of the LQC<sub>x</sub>  $\mathcal{I}(\rho_{i,i+1}, \sigma_i^x)$ ; (b) two-qubit correlation function  $\langle \sigma_i^x \sigma_{i+1}^y \rangle$ ; the color map represents the strength of the correlation function. The white zone in the AFM phase and the factorization line and the factorization region, respectively. Parameters:  $D = 0.2$ ,  $\Delta = 0.2$ , and  $J = 1$ .

romagnetic) phase [26]. In the following, we concentrate on the planar regime ( $|\Delta| < 1$ ). Figure 5 shows the corresponding behavior of the entanglement and the quantum coherence with  $\gamma = 0.6$ ,  $\Delta = 0.2$  and  $D = 0.2$ . One observes that comparing with Fig. 3, the presence of the term  $\propto \Delta$  merely increases the values of field at the critical point  $h_c$  and the factorized point  $h_f$ . Meanwhile, the hopping parameters  $\mu$  and  $t$  are found to be complex, but the pairing parameter  $\delta$  remains a real number, as is disclosed in Fig. 6.

The first-order derivative of the LQC<sub>z</sub> still follows a logarithmic divergence across the critical point, as is shown in the inset of Fig. 7. The calculations are summarized by the ground-state phase diagram shown in

Fig. 8(a). One finds that  $\langle \sigma_i^x \sigma_{i+1}^y \rangle = 0$  in the gapped phase [see Fig. 8(b)], and these three self-consistent parameters are found to be real numbers as a function of  $h$ . On the other hand, when the system is in the gapless phase,  $\langle \sigma_i^x \sigma_{i+1}^y \rangle$  becomes finite. Such a feature implies that  $\langle \sigma_i^x \sigma_{i+1}^y \rangle$  is an order parameter to identify the chiral phase for general Heisenberg XYZ model.

## V. CONCLUSION AND SUMMARY

In this article, we studied the one-dimensional XYZ model with Dzyaloshinskii-Moriya interaction, which induces a gapless chiral phase. We point out a few differences in deriving the exact correlation functions in this chiral phase and the associated density matrix in systems with broken reflection symmetry, which then give rise to the misleading message about the quantum criticality. We firstly scrutinize the limiting situation, where the XY chain is rigorously solvable by applying the Jordan-Wigner transformation. Knowledge of exact solutions endowed with precisely determined properties of separability or criticality can be of great relevance in the study of general cases, that are not exactly solvable. For models not admitting exact general solutions, we carry on an analytical approach that combines a Jordan-Wigner transformation with a mean-field approximation. We find the Wigner-Yanase skew information as a quantum coherence witness which may well identify the quantum phase transitions.

Besides, the logarithmic scaling behavior for the information measures are found around quantum criticality. Quantum coherence arising from the quantum superposition acts as one of perspective towards a kaleidoscope of quantum correlations, and it is the key resource for applications of quantum technology besides entanglement and other types of quantum correlations. We have seen that the ground states of complex quantum systems are typically entangled. Nevertheless, for some specific values of the parameters, a ground state may be completely separable.

We also discussed the occurrence of the separable ground state in the antiferromagnetic phase, which is marked by the vanishing of the concurrence. Such factorization points can be also sensed by the discontinuous jump of the first derivative of the Wigner-Yanase skew information measure. In the gapless chiral phase, the factorization line becomes the factorization volume, which is implied by the extinguishment of ground-state pairwise concurrence. A merit of the concurrence and local quantum coherence is that the property emerges for a finite chain, in contrast to the signal of global entanglement can be observed in the thermodynamics limit after taking the phase-flip symmetry breaking into account [57]. As most multipartite measures are exhaustively expensive to obtain, the bipartite measures are comparably easy to calculate, and especially can be determined without a full tomography of the state. Nevertheless, the vanishing



concurrence is a necessary condition for the occurrence of a completely separable state, and hence a confirmative conclusion desires further investigations.

### ACKNOWLEDGMENTS

W.-L. You acknowledges NSFC under Grant No. 11474211. N. Wu acknowledges NSFC under Grant No. 11705007. A. M. Oleś kindly acknowledges support by Narodowe Centrum Nauki (NCN, Poland) under Project No. 2016/23/B/ST3/00839 and is grateful for the Alexander von Humboldt Foundation Fellowship (Humboldt-Forschungspreis).

### Appendix A: Exact solution of XY chain and correlations

For  $\Delta = 0$ , the diagonalization procedure of the Heisenberg model (1) includes the well-established techniques of Jordan-Wigner and Bogoliubov transformations. We use Jordan-Wigner transformation, i.e.,

$$\sigma_j^+ \equiv \frac{1}{2}(\sigma^x + i\sigma^y) = e^{i\pi \sum_{n < j} c_n^\dagger c_n} c_j, \quad (\text{A1})$$

to covert the spin operators to fermion operators. As a result, the Hamiltonian (1) can be written as the quadratic form of the creation operator and the annihilation operator of spinless fermions ( $J=1$  is assumed in the following),

$$\mathcal{H} = \sum_{j=1}^N [(1 + 2iD)c_{j+1}^+ c_j + (1 - 2iD)c_j^+ c_{j+1} + \gamma(c_{j+1}c_j + c_j^+ c_{j+1}^+) - h(1 - 2c_j^+ c_j)]. \quad (\text{A2})$$

In the next step we adopt Fourier transformation to express Eq. (A2) in the momentum space. Then by successive application of the Bogoliubov transformation, this Hamiltonian can be reduced to a diagonal form:

$$\mathcal{H} = \sum_{k=-\pi}^{\pi} \epsilon_k \left( f_k^\dagger f_k - \frac{1}{2} \right), \quad (\text{A3})$$

where

$$\epsilon_k = -4D \sin k + 2\sqrt{(\cos k + h)^2 + (\gamma \sin k)^2}. \quad (\text{A4})$$

The ground state  $|\Psi_0\rangle$  follows the total filling of the Fermi-Dirac statistics, and the lowest energy is obtained when all the states with negative energies ( $\epsilon_k < 0$ ) are filled by fermions and the ones with positive energies ( $\epsilon_k \geq 0$ ) are empty. With Eq. (A4), the gap  $\Delta \equiv \min_k \epsilon_k$  closes at the critical mode  $k_c$  and the critical field  $h_c$ , and then we have

$$\begin{aligned} h &= -\cos k + i\sqrt{\gamma^2 - 4D^2} \sin k, & \text{for } \gamma > 2D, \\ h &= -\cos k + \sqrt{4D^2 - \gamma^2} \sin k, & \text{for } \gamma \leq 2D. \end{aligned}$$

The reality of  $h_c$  requires that  $h_c = 1$  and  $k_c = \pi$  are the solutions for  $\gamma > 2D$ , while for  $\gamma \leq 2D$  there are solutions with arbitrary  $k$ , suggesting the system is always gapless for  $h < \sqrt{4D^2 - \gamma^2} + 1$ . The analysis suggests the critical lines are  $h = 1$ ,  $\gamma = 2D$ , and  $h = \sqrt{4D^2 - \gamma^2} + 1$ , respectively.

The phase diagram at finite DM interaction and finite magnetic field consists of three phases: AFM phase, PM phase, and the gapless chiral phase. The transition from AFM phase to PM phase for  $\gamma > 2D$  is similar to the conventional order-disorder transition in the transverse Ising model for  $\gamma = 1$  and  $D = 0$ . They are in the same universality class. The AFM phase disappears only when  $\gamma = 0$ . With  $D$  getting smaller, the chiral phase shrinks. When the DM interaction is large ( $\gamma < 2D$ ), part of the spectrum becomes negative and the energy gap disappears, with two Fermi points  $k_L$  and  $k_R$  given by

$$k_{L,R} = \cos^{-1} \left[ \frac{-h \pm \sqrt{(4D^2 - \gamma^2)(4D^2 - \gamma^2 + 1 - h^2)}}{4D^2 - \gamma^2 + 1} \right]. \quad (\text{A5})$$

For  $k_L \leq k \leq k_R$ , the excitation spectrum  $\epsilon_k$  becomes negative, and these modes in the ground state  $|\psi_0\rangle$  are occupied by electrons, namely  $f_k^\dagger |\psi_0\rangle = 0$  [93]. The system enters the gapless chiral phase. As the magnetic field  $h$  increases, the system changes from the chiral phase to the PM phase.

In order to identify different phases, we choose correlation function between two lattice sites as the order parameter, which can be used to describe the nature of the ground state. The correlation function can be defined as:  $G_{i,j}^{\alpha\beta} \equiv \langle \sigma_i^\alpha \sigma_j^\beta \rangle - \langle \sigma_i^\alpha \rangle \langle \sigma_j^\beta \rangle$ , here  $\alpha, \beta = x, y, z$ . Since the system is translation-invariant, the value of the correlation function is only related to the relative distance between the position of the two sites (such as  $i$  and  $j$ ), so  $G_{i,j}^{\alpha\beta}$  can be abbreviated as  $G_r^{\alpha\beta}$ , here  $r = i - j$ . For general  $\langle \sigma_i^x \sigma_j^x \rangle$ ,  $\langle \sigma_i^y \sigma_j^y \rangle$ , the expanded form can be expressed as a form of Pfaffian [94]. In other words, it can be written as the determinant of the  $2n \times 2n$  ( $n \equiv |j - i|$ ) dimension anti-symmetric matrix.

It is illuminating to discuss the asymptotic behavior of the correlation functions in the exact case. Barouch and McCoy studied the magnetization and the correlation function of XY chain in a transverse field [92, 94]. It considered the non-zero temperature correlations of the horizontal-field XX model [95]. The research shows that the asymptotic behavior of the correlation function ( $r \rightarrow \infty$ ) can be written in Ornstein-Zernike form specially in the context of 1D systems significantly away from the critical points [96, 97]

$$G_r^{xx} \sim A r^{1-\eta_x} \exp(-r/\xi), \quad (\text{A6})$$

where  $A$  is a form factor,  $\langle \sigma_i^x \rangle$  is the magnetization in the  $x$  direction and  $\xi$  is the correlation length.  $\eta_x$  is the Tomonaga-Luttinger exponents for the  $x$  spin component

[98], which is in the algebraic behavior is equal to 1/2 for such an asymptotic behavior of the correlation function [99]. In all cases  $(-1)^r G_r^{xx}$  vanishes exponentially rapidly as  $r \rightarrow \infty$  for all  $h$  and  $\gamma$ .

However, the rate of this exponential vanishing depends on  $h$ , and this dependence is qualitatively different in different regions. When  $|h| > 1$ , the system is in the paramagnetic state and the magnetization in the  $x$  direction disappears, namely,  $\langle \sigma_i^x \rangle = 0$ , and at this time  $\lim_{r \rightarrow \infty} G_r^{xx} \sim (-1)^r r^{-1/2} \exp(-r/\xi)$ ,  $\lim_{r \rightarrow \infty} G_r^{yy} \sim (-1)^r r^{-3/2} \exp(-r/\xi)$ . When  $|h| \leq 1$ ,  $\lim_{r \rightarrow \infty} G_r^{xx} = (-1)^r 2[\gamma^2(1-h^2)]^{1/4}(1+\gamma)^{-1}$ . This means that when  $\gamma \neq 0$ , there is a long range order. When  $\gamma = 0$ , the long range order does not exist. In the Ising limit,  $\lim_{r \rightarrow 0} G_r^{xx} = (-1)^r (1-h^2)^{1/4}$ . This implies that the critical exponent  $\beta$  is 1/8 for the Ising transition (approaching the transition as a ferromagnet) and 1/4 for the anisotropic transition.  $G_r^{xx}$  decreases to zero rapidly with the increasing of  $r$  in the paramagnetic phase, while  $G_r^{xx}$  remains a constant with the change of  $r$  in the AFM phase.

At the critical point of Ising transition ( $h = 1$ ),  $G_r^{xx} \sim r^{-1/4}$ , the critical exponent  $\eta_x = 5/4$ .  $G_r^{yy} \sim r^{-9/4}$  with  $\eta_y = 13/4$ . At the anisotropic phase transition line when  $h = 0$  and  $\gamma = 0$ ,  $G_r^{xx} \sim r^{-1/2}$  [98]. The DM interactions cause the correlation function  $G_r^{xy}$  to decrease oscillatory with the increase of the distance  $r$ . When  $\gamma = 0$ , the correlation function  $G_r^{xy}$  oscillates more violently than  $\gamma = 1$  with the increase of the distance  $r$ .

For specific values of the anisotropy parameter and the relative strengths of the uniform transverse magnetic fields, the ground state of this model is known to be doubly degenerate and factorizable along two hyperbolic

lines, known as the factorization lines. For the factorization points  $h^2 + \gamma^2 = 1$  with  $D = 0$ , we can obtain an explicit form for all  $r$ :  $\langle \sigma_j^x \sigma_{j+r}^x \rangle = (-1)^r 2\gamma/(1+\gamma)$ ,  $\langle \sigma_j^y \sigma_{j+r}^y \rangle = 0$ ,  $\langle \sigma_j^z \sigma_{j+r}^z \rangle = \langle \sigma_j^z \rangle^2$ .

## Appendix B: Fermionic mean-field approximation

According to the mean-field decomposition in Eq. (5), the order parameters are defined as

$$\beta_1 = \langle c_j^\dagger c_j \rangle, \quad (\text{B1})$$

$$\beta_2 = \langle c_j^\dagger c_{j+1} \rangle, \quad (\text{B2})$$

$$\beta_3 = \langle c_j c_{j+1} \rangle. \quad (\text{B3})$$

The energy spectrum (A4) can be rewritten as

$$\varepsilon(k) = -4D \sin(k) + 2\sqrt{\tau(k)^2 + \varphi(k)^2}, \quad (\text{B4})$$

where  $\tau(k) = J[(1-4\Delta\beta_2) \cos(k) + 2\Delta(2\beta_1-1)] + h$  and  $\varphi(k) = J(\gamma - 4\Delta\beta_3) \sin(k)$ . To this end, one finds the solutions could be retrieved by self-consistently solving the following equations:

$$\beta_1 = \sum_{k=-\pi}^{\pi} \left[ \frac{\varphi(k)^2 \theta(-\varepsilon_k) + \varsigma(k)^2 \theta(\varepsilon_k)}{\varphi(k)^2 + \varsigma(k)^2} \right], \quad (\text{B5})$$

$$\beta_2 = \sum_{k=-\pi}^{\pi} \left[ \frac{\varphi(k)^2 \theta(-\varepsilon_k) + \varsigma(k)^2 \theta(\varepsilon_k)}{\varphi(k)^2 + \varsigma(k)^2} e^{-ik} \right], \quad (\text{B6})$$

$$\beta_3 = \sum_{k=-\pi}^{\pi} \left[ \frac{-\theta(-\varepsilon_k) + \theta(\varepsilon_k)}{\varphi(k)^2 + \varsigma(k)^2} (i\varphi(k)\varsigma(k)) e^{ik} \right], \quad (\text{B7})$$

with  $\varsigma(k) = \tau(k) + \sqrt{\tau(k)^2 + \varphi(k)^2}$ .

- 
- [1] S. Sachdev, *Quantum Phase Transition* (Cambridge University Press, Cambridge, England, 1999).
- [2] M.-J. Hwang, R. Puebla, and M. B. Plenio, Phys. Rev. Lett. **115**, 180404 (2015).
- [3] M.-J. Hwang and M. B. Plenio, Phys. Rev. Lett. **117**, 123602 (2016).
- [4] M. Liu, S. Chesi, Z.-J. Ying, X. Chen, H.-G. Luo, and H.-Q. Lin, Phys. Rev. Lett. **119**, 220601 (2017).
- [5] J. Larson and E. K. Irish, J. Phys. A: Math. Theor. **50**, 174002 (2017).
- [6] Y. M. Wang, W.-L. You, M. X. Liu, Y.-L. Dong, H.-G. Luo, G. Romero, and J. Q. You, New J. Phys. **20**, 053061 (2018).
- [7] J. Åberg, Phys. Rev. Lett. **113**, 150402 (2014).
- [8] V. Narasimhachar and G. Gour, Nat. Commun. **6**, 7689 (2015).
- [9] P. Źwikliński, M. Studziński, M. Horodecki, and J. Oppenheim, Phys. Rev. Lett. **115**, 210403 (2015).
- [10] M. Lostaglio, D. Jennings, and T. Rudolph, Nature Commun. **6**, 6383 (2015).
- [11] M. Lostaglio, K. Korzekwa, D. Jennings, and T. Rudolph, Phys. Rev. X **5**, 021001 (2015).
- [12] E. Schrödinger, Math. Proc. Cambridge Philos. Soc. **31**, 555 (1935).
- [13] W.-L. You, A. M. Oleś, and P. Horsch, New J. Phys. **17**, 083009 (2015).
- [14] T. Baumgratz, M. Cramer, and M. B. Plenio, Phys. Rev. Lett. **113**, 140401 (2014).
- [15] A. Streltsov, U. Singh, H. S. Dhar, M. N. Bera, and G. Adesso, Phys. Rev. Lett. **115**, 020403 (2015).
- [16] D. Braun, G. Adesso, F. Benatti, R. Floreanini, U. Marzolino, M. W. Mitchell, and S. Pirandola, Rev. Mod. Phys. **90**, 035006 (2018).
- [17] J.-J. Chen, J. Cui, Y.-R. Zhang, and H. Fan, Phys. Rev. A **94**, 022112 (2016).
- [18] W.-L. You, C.-J. Zhang, W. Ni, M. Gong, and A. M. Oleś, Phys. Rev. B **95**, 224404 (2017).
- [19] P. Zanardi, H. T. Quan, X. Wang, and C. P. Sun, Phys. Rev. A **75**, 032109 (2007).
- [20] W.-L. You, Y.-W. Li, and S.-J. Gu, Phys. Rev. E **76**, 022101 (2007).
- [21] J. Kurmann, H. Thomas, and G. Müller, Physica A **112**, 235 (1982).
- [22] R. Horodecki, P. Horodecki, M. Horodecki, and K. Horodecki, Rev. Mod. Phys. **81**, 865 (2009).
- [23] L. M. K. Vandersypen and I. L. Chuang, Rev. Mod. Phys.

- 76**, 1037 (2005).
- [24] I. M. Georgescu, S. Ashhab, and F. Nori, *Rev. Mod. Phys.* **86**, 153 (2014).
- [25] W.-L. You, G.-H. Liu, P. Horsch, and A. M. Oleś, *Phys. Rev. B* **90**, 094413 (2014).
- [26] P. Thakur and P. Durganandini, *Phys. Rev. B* **97**, 064413 (2018).
- [27] M. Brockmann, A. Klümper, and V. Ohanyan, *Phys. Rev. B* **87**, 054407 (2013).
- [28] C. Radhakrishnan, I. Ermakov, and T. Byrnes, *Phys. Rev. A* **96**, 012341 (2017).
- [29] C. Radhakrishnan, M. Parthasarathy, S. Jambulingam, and T. Byrnes, *Phys. Rev. Lett.* **116**, 150504 (2016).
- [30] S.-P. Li and Z.-H. Sun, *Phys. Rev. A* **98**, 022317 (2018).
- [31] D. Porrás and J. I. Cirac, *Phys. Rev. Lett.* **92**, 207901 (2004).
- [32] N. G. Berloff, M. Silva, K. Kalinin, A. Askitopoulos, J. D. Töpfer, P. Cilibrizzi, W. Langbein, and P. G. Lagoudakis, *Nature Mater.* **16**, 1120 (2017).
- [33] I. Dzyaloshinskii, *J. Phys. Chem. Solids* **4**, 241 (1958).
- [34] T. Moriya, *Phys. Rev.* **120**, 91 (1960).
- [35] S. Seki, X. Z. Yu, S. Ishiwata, and Y. Tokura, *Science* **336**, 198 (2012).
- [36] T. Adams, A. Chacon, M. Wagner, A. Bauer, G. Brandl, B. Pedersen, H. Berger, P. Lemmens, and C. Pfleiderer, *Phys. Rev. Lett.* **108**, 237204 (2012).
- [37] J. H. Yang, Z. L. Li, X. Z. Lu, M.-H. Whangbo, S.-H. Wei, X. G. Gong, and H. J. Xiang, *Phys. Rev. Lett.* **109**, 107203 (2012).
- [38] M. Matsuda, R. S. Fishman, T. Hong, C. H. Lee, T. Ushiyama, Y. Yanagisawa, Y. Tomioka, and T. Ito, *Phys. Rev. Lett.* **109**, 067205 (2012).
- [39] P. Wang, Z.-Q. Yu, Z. Fu, J. Miao, L. Huang, S. Chai, H. Zhai, and J. Zhang, *Phys. Rev. Lett.* **109**, 095301 (2012).
- [40] L. W. Cheuk, A. T. Sommer, Z. Hadzibabic, T. Yefsah, W. S. Bakr, and M. W. Zwierlein, *Phys. Rev. Lett.* **109**, 095302 (2012).
- [41] K. Jiménez-García, L. J. LeBlanc, R. A. Williams, M. C. Beeler, A. R. Perry, and I. B. Spielman, *Phys. Rev. Lett.* **108**, 225303 (2012).
- [42] W. S. Cole, S. Zhang, A. Paramekanti, and N. Trivedi, *Phys. Rev. Lett.* **109**, 085302 (2012).
- [43] Y. Tokura and S. Seki, *Adv. Mater.* **22**, 1554 (2010).
- [44] I. A. Sergienko and E. Dagotto, *Phys. Rev. B* **73**, 094434 (2006).
- [45] L. Shekhtman, O. Entin-Wohlman, and A. Aharony, *Phys. Rev. Lett.* **69**, 836 (1992).
- [46] H. A. Bethe, *Z. Phys.* **71**, 205 (1931).
- [47] C. N. Yang and C. P. Yang, *Phys. Rev.* **150**, 321 (1966).
- [48] G. Vionnet, B. Kumar, and F. Mila, *Phys. Rev. B* **95**, 174404 (2017).
- [49] J. Carrasquilla and R. Melko, *Nat. Phys.* **13**, 431 (2017).
- [50] L. Wang, *Phys. Rev. B* **94**, 195105 (2016).
- [51] S. J. Wetzel, *Phys. Rev. E* **96**, 022140 (2017).
- [52] W. Hu, R. R. P. Singh, and R. T. Scalettar, *Phys. Rev. E* **95**, 062122 (2017).
- [53] C. Wang and H. Zhai, *Phys. Rev. B* **96**, 144432 (2017).
- [54] M. J. S. Beach, A. Golubeva, and R. G. Melko, *Phys. Rev. B* **97**, 045207 (2018).
- [55] C. Wang and H. Zhai, *Frontiers of Physics* **13**, 130507 (2018).
- [56] W. Zhang, J. Liu, and T.-C. Wei, *Phys. Rev. E* **99**, 032142 (2019).
- [57] R. Radgohar and A. Montakhab, *Phys. Rev. B* **97**, 024434 (2018).
- [58] R. Toskovic, R. van den Berg, A. Spinelli, I. S. Eliens, B. van den Toorn, B. Bryant, J. S. Caux, and A. F. Otte, *Nature Phys.* **12**, 656 (2016).
- [59] S.-B. Zheng and G.-C. Guo, *Phys. Rev. Lett.* **85**, 2392 (2000).
- [60] M. Christandl, N. Datta, A. Ekert, and A. J. Landahl, *Phys. Rev. Lett.* **92**, 187902 (2004).
- [61] S. Bose, *Phys. Rev. Lett.* **91**, 207901 (2003).
- [62] S. M. Giampaolo, G. Adesso, and F. Illuminati, *Phys. Rev. Lett.* **100**, 197201 (2008).
- [63] B.-L. Ye, B. Li, Z.-X. Wang, X. Li-Jost, and S.-M. Fei, *Sci. China-Phys. Mech. Astron.* **61**, 110312 (2018).
- [64] B. Q. Liu, B. Shao, J. G. Li, J. Zou, and L. A. Wu, *Phys. Rev. A* **83**, 052112 (2011).
- [65] Y.-C. Li and S.-S. Li, *Phys. Rev. A* **79**, 032338 (2009).
- [66] D. Lu, T. Xin, N. K. Yu, Z. F. Ji, J. X. Chen, G. L. Long, J. Baugh, X. H. Peng, B. Zeng, and R. Laflamme, *Phys. Rev. Lett.* **116**, 230501 (2016).
- [67] W.-L. You, Y.-C. Qiu, and A. M. Oleś, *Phys. Rev. B* **93**, 214417 (2016).
- [68] S. Lei and P. Tong, *Physica B* **463**, 1 (2015).
- [69] E. P. Wigner and M. M. Yanase, *Proc. Natl. Acad. Sci. (U.S.A.)* **49**, 910 (1963).
- [70] D. Girolami, *Phys. Rev. Lett.* **113**, 170401 (2014).
- [71] S. L. Luo, S. S. Fu, C. H. Oh, *Phys. Rev. A* **85**, 032117 (2012).
- [72] G. Karpat, B. Cakmak, and F. F. Fanchini, *Phys. Rev. B* **90**, 104431 (2014).
- [73] W. K. Wootters, *Phys. Rev. Lett.* **80**, 2245 (1998).
- [74] T. Werlang, S. Souza, F. F. Fanchini, and C. J. Villas Boas, *Phys. Rev. A* **80**, 024103 (2009).
- [75] T.-C. Yi, Y.-R. Ding, J. Ren, Y.-M. Wang, W.-L. You, *Acta Phys. Sin.* **67**, 140303 (2018).
- [76] M.-L. Hu, X.-Y. Hu, J.-C. Wang, Y. Peng, Y.-R. Zhang, and H. Fan, *Phys. Rep.* **07**, 004 (2018).
- [77] W. K. Wootters and W. H. Zurek, *Nature (London)* **299**, 802 (1982).
- [78] A. Osterloh, L. Amico, G. Falci, and R. Fazio, *Nature (London)* **416**, 608 (2002).
- [79] T. J. Osborne and M. A. Nielsen, *Phys. Rev. A* **66**, 032110 (2002).
- [80] S.-J. Gu, H.-Q. Lin, and Y.-Q. Li, *Phys. Rev. A* **68**, 042330 (2003).
- [81] G. Vidal, J. I. Latorre, E. Rico, and A. Kitaev, *Phys. Rev. Lett.* **90**, 227902 (2003).
- [82] H. Ollivier and W. H. Zurek, *Phys. Rev. Lett.* **88**, 017901 (2001).
- [83] M. N. Barber, in: *Phase Transitions and Critical Phenomena* (Academic, London, 1983), Vol. **8**, 146-259.
- [84] S. L. Zhu, *Phys. Rev. Lett.* **96**, 077206 (2006).
- [85] S. G. Lei and P. Q. Tong, *Quantum Inf. Process* **15**, 1811 (2016).
- [86] S. Campbell, J. Richens, N. L. Gullo, and T. Busch, *Phys. Rev. A* **88**, 062305 (2013).
- [87] T.-C. Wei, D. Das, S. Mukhopadhyay, S. Vishveshwara, and P. M. Goldbart, *Phys. Rev. A* **71**, 060305(R) (2005).
- [88] G. Müller and R. E. Shrock, *Phys. Rev. B* **32**, 5845 (1985).
- [89] T. Roscilde, P. Verrucchi, A. Fubini, S. Haas, and V. Tognetti, *Phys. Rev. Lett.* **94**, 147208 (2005).
- [90] M. Cerezo, R. Rossignoli, and N. Canosa, *Phys. Rev. A* **94**, 042335 (2016).
- [91] M. Cerezo, R. Rossignoli, N. Canosa, and E. Ríos, *Phys.*

- Rev. Lett. **119**, 220605 (2017).
- [92] E. Barouch and B. M. McCoy, Phys. Rev. A **2**, 1075 (1970).
- [93] M. Zhong, H. Xu, X. X. Liu, and P. Q. Tong, Chin. Phys. B **22**, 090313 (2013).
- [94] E. Barouch and B. M. McCoy, Phys. Rev. A **3**, 786 (1971).
- [95] A. R. Its, A. G. Izergin, V. E. Korepin, and N. A. Slavnov, Phys. Rev. Lett. **70**, 1704 (1993).
- [96] T. Vekua and G. Sun, Phys. Rev. B **94**, 014417 (2016).
- [97] D. P. Landau and K. Binder, *A Guide to Monte Carlo Simulations in Statistical Physics* (Cambridge University Press, 2005).
- [98] J. E. Bunder and R. H. McKenzie, Phys. Rev. B **60**, 344 (1999).
- [99] M. M. Rams, V. Zauner, M. Bal, J. Haegeman, and F. Verstraete, Phys. Rev. B **92**, 235150 (2015).